PHYSICAL REVIEW E **79**, 020601(R) (2009)

Method for computing short-range forces between solid-liquid interfaces driving grain boundary premelting

J. J. Hoyt,[1] David Olmsted,[2] Saryu Jindal,[3] Mark Asta,[3] and Alain Karma[4]
[1]*Department of Materials Science and Engineering, McMaster University, Hamilton, Ontario, Canada L8S 4L7*
[2]*Sandia National Laboratories, Albuquerque, New Mexico 87185, USA*
[3]*Department of Chemical Engineering and Materials Science, University of California, Davis, California 95616, USA*
[4]*Department of Physics and Center for Interdisciplinary Research on Complex Systems, Northeastern University, Boston, Massachusetts 02115, USA*

(Received 21 October 2008; published 13 February 2009)

We present a molecular dynamics based method for accurately computing short-range structural forces resulting from the overlap of spatially diffuse solid-liquid interfaces at wetted grain boundaries close to the melting point. The method is based on monitoring the fluctuations of the liquid layer width at different temperatures to extract the excess interfacial free energy as a function of this width. The method is illustrated for a high-energy $\Sigma 9$ twist boundary in pure Ni. The short-range repulsion driving premelting is found to be dominant in comparison to long-range dispersion and entropic forces and consistent with previous experimental findings that nanometer-scale layer widths may be observed only very close to the melting point.

DOI: 10.1103/PhysRevE.79.020601 PACS number(s): 68.08.Bc, 61.72.Mm, 64.70.D−

The term "premelting" refers to the formation of a thin, thermodynamically stable, liquidlike film at an interface for temperatures below the equilibrium melting point (T_M). Premelting at grain boundaries (GBs) can have dramatic consequences in the context of materials processing and the physical properties of polycrystals at high homologous temperatures. Despite the importance of this phenomenon, direct experimental observations of GB premelting remain relatively rare [1–3], particularly in the case of pure materials [2,3]. Consequently, outstanding fundamental questions remain concerning the nature of the forces which drive premelting at these internal interfaces. In this Rapid Communication, we introduce a molecular dynamics (MD) method that exploits large fluctuations in GB width to compute short-range forces resulting from the overlap of spatially diffuse crystal-melt interfaces from two grains of different orientations. We demonstrate the application of this method in a direct calculation of the excess free energy of the GB as a function of this width for a high-energy boundary in a classical model of elemental Ni. The results yield quantitative insights into the relative magnitudes of these short-range structural forces and other long-ranged contributions, and help explain the origins of the experimental observations [3] that GB premelting in pure metals may occur only over extremely small temperature ranges near T_M.

Premelting generally reflects a competition between opposing bulk and interfacial thermodynamic factors, giving rise to a free energy (per unit area) of the following form (e.g., [4]):

$$G(w) = \Delta G_f w + \Psi(w). \tag{1}$$

In Eq. (1) w represents the width of the premelted layer, ΔG_f is the free energy difference between solid and liquid (per unit volume) that penalizes the formation of liquid films below T_M, and $\Psi(w)$ is the so-called "disjoining potential," which takes the limits of γ_{GB} (the interfacial free energy of a "dry" grain boundary) and $2\gamma_{SL}$ (twice the solid-liquid interfacial free energy) for zero and infinite w, respectively. In general, the disjoining potential contains both repulsive and attractive contributions. Long-ranged dispersion forces lead to an attractive interaction between solid-liquid interfaces [4,5] which are dominant at large w and are predicted to give rise to finite interfacial widths at T_M [4]. For $\Delta\gamma = \gamma_{GB} - 2\gamma_{SL} > 0$, a repulsive contribution to $\Psi(r)$ arises from short-ranged structural interactions (Ψ_{SR}), associated with the overlap of the diffuse regions of the solid-liquid interfaces. The exact nature of this structural contribution remains less well understood.

Previous theoretical analyses [6–8] have considered an exponentially decaying form for the short-ranged contribution to the disjoining potential:

$$\Psi_{SR}(w) = 2\gamma_{SL} + \Delta\gamma \exp(-w/\delta) \tag{2}$$

which was also derived from a lattice gas model [9]. Here δ is an interaction length on the order of the atomic spacing. Insertion of Eq. (2) into Eq. (1) leads to the prediction of a continuous premelting transition with an equilibrium grain boundary width that diverges logarithmically as T_M is approached from below. For rough interfaces considered in the current study, Ψ_{SR} contains a "bare" contribution (in the language of [8]), which is renormalized by capillary fluctuations. Such capillary fluctuations also give rise to an additional repulsive entropic contribution to the disjoining potential, associated with the long-wavelength fluctuations of the two interfaces for large separation [7]. For two-dimensional interfaces this term produces only a subdominant short-range force, and a straightforward estimate of its magnitude using analytical results from the literature [7] and the parameters for Ni from MD results below show that this entropic force is completely negligible in comparison to the contribution from Eq. (2). This additional entropic contribution will thus be neglected for the remainder of the paper.

Recent theoretical results suggest that the nature of Ψ_{SR} can be much more complex than indicated by Eq. (2).

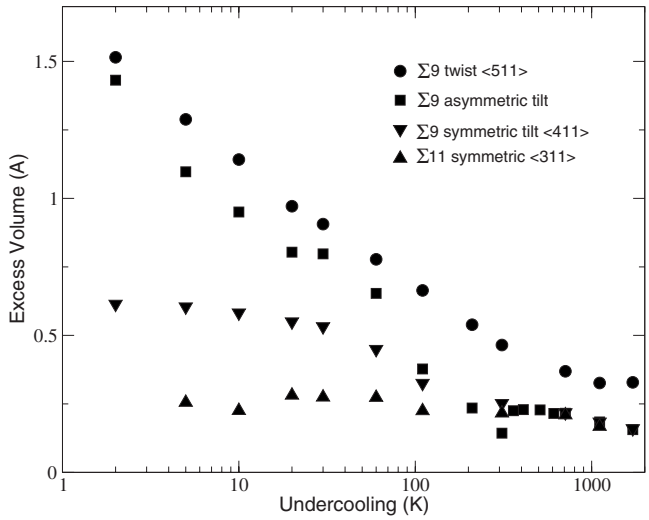

FIG. 1. Calculated excess volumes versus temperature for four grain boundaries in elemental Ni.

Diffuse-interface theories [10,11], which neglect long-ranged forces and capillary fluctuations, have shown that the dependence of w on temperature may in some cases display a discontinous jump, with the coexistence of wet and dry interface states, while other parameter choices lead to continuous increases in w up to T_M. In recent applications of the phase-field crystal (PFC) method to the study of grain boundary premelting [12,13], results for two-dimensional hexagonal systems give a disjoining potential that is purely repulsive above a critical misorientation [12], even though the PFC model does not contain long-range dispersion interactions. While theoretical models thus suggest a rich behavior for the disjoining potential in general, they are presently unable to predict the absolute magnitude of this contribution in specific systems, and it remains unclear for which GB misorientations the various qualitative forms for Ψ_{SR} may be expected in real materials. To facilitate further progress in the understanding of the forces that drive premelting, we describe in the remainder of this Rapid Communication a quantitative framework for the direct calculation of $\Psi_{SR}(w)$, through histogram analyses of interface widths derived from MD.

Classical MD simulations provide a framework ideally suited for probing the short-ranged structural contributions to $\Psi(w)$. Such simulations have been employed extensively in the past to study GB premelting [15,16] and in the present work we propose a methodology to extend the analysis of such MD results as a framework for extracting $\Psi(w)$. We demonstrate the approach for a classical model of elemental Ni, described by the embedded-atom potential of Foiles, Baskes, and Daw [18]. The potential was chosen as we have previously calculated the solid-liquid interfacial free energies, melting temperature, and solid-liquid thermodynamic properties with high precision. A value for γ_{SL} of 285 mJ/m^2 for the potential has been determined using the capillary fluctuation method [17], and a coexistence technique was used to compute a melting temperature of 1710 ± 5 K [19] (from subsequent coexistence runs and the data presented below the uncertainty in this estimate has been reduced to approximately 1 K). We began by considering a total of four boundaries with a range of zero-temperature grain boundary energies spanning 450 to 1430 mJ/m^2, which is 0.8–2.5 times the value of $2\gamma_{SL}$. For each GB we performed a conjugate gradient minimization (exploring also the microscopic translational degrees of freedom and the excess number of atoms at the grain boundary) to derive an optimized zero-temperature interface structure. With this structure as a starting point, the GBs were heated gradually up to the melting point, employing constant-temperature MD simulations (details of the procedures will be presented elsewhere).

Figure 1 shows the calculated excess volume of each GB, displaying three qualitatively different behaviors. The highest-energy boundaries feature an excess volume displaying a logarithmic divergence characteristic of a continuous premelting transition. The lower-energy GBs show two different behaviors. In one case the excess volume rises with increasing temperature but then plateaus, maintaining a finite excess volume at the melting temperature. The lowest-energy GB shows an excess volume that is relatively small and only weakly dependent on temperature. The range of behavior demonstrated by the different GBs in Fig. 1 is qualitatively similar to that seen in very recent GB simulations for Si [16].

For the remainder of this Rapid Communication we focus on one of the two high-energy boundaries displaying clear premelting behavior, namely, the $\Sigma 9$ boundary characterized

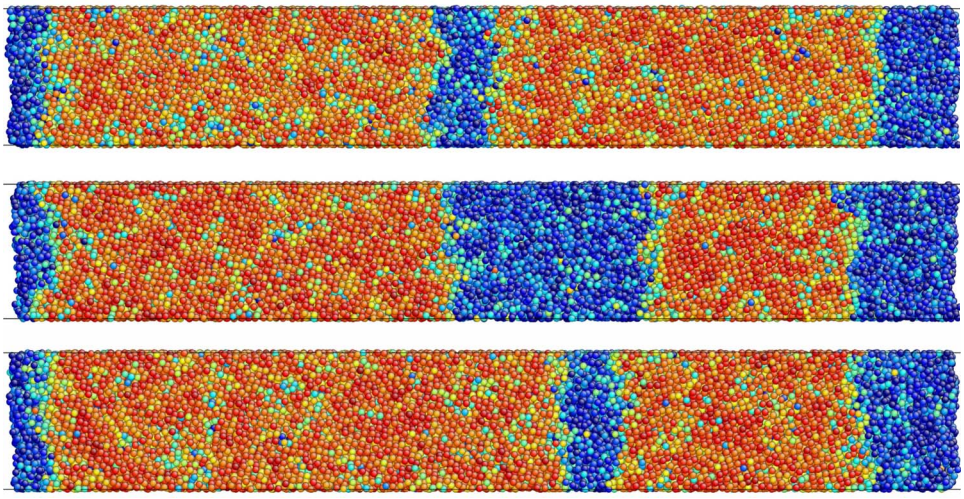

FIG. 2. (Color online) Snapshots from a MD simulation at an undercooling of 2 K, illustrating the dynamic nature of the GB width. The red (blue) areas indicate regions of solid- (liquid)like liquid order. The liquidlike regions at the far left- and right-hand sides represent premelting of the free surfaces of the simulation cell, while that in the middle corresponds to the premelted grain boundary.

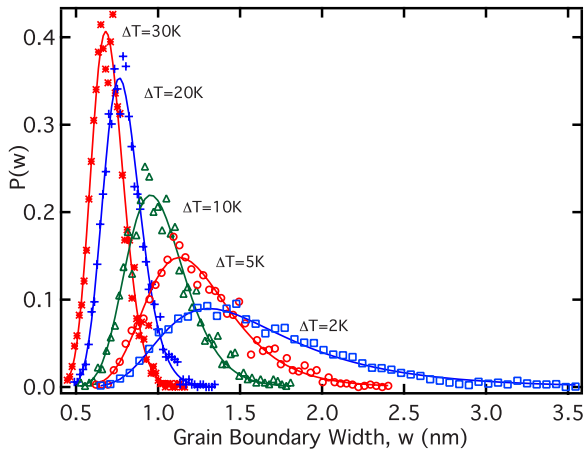

FIG. 3. (Color online) Distribution function $P(w)$ vs w from the MD simulations (symbols) versus the least-squares fits of the premelting model of Eqs. (1) and (2).

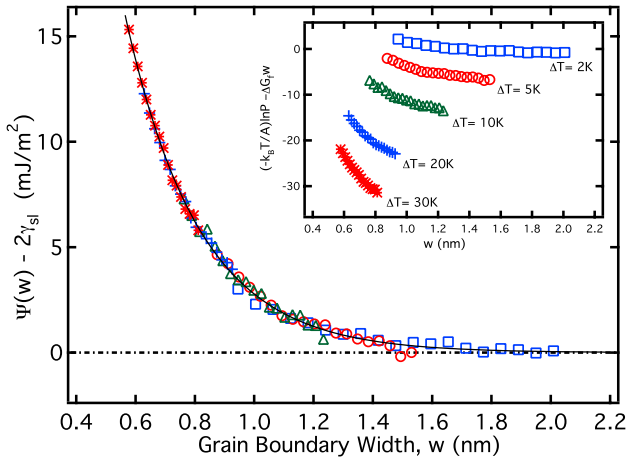

FIG. 4. (Color online) Illustration of the histogram method used to extract the disjoining potential. The inset plots the right-hand side of Eq. (4) with the constants a_i set to zero. The main plot merges the individual histograms of data and reproduces the complete disjoining potential $\Psi(w)$. The solid line is a best fit to the exponential decay given in Eq. (2).

by a 120° rotation about the GB normal lying along the [511] crystallographic direction. We study the structural properties of the grain boundary at five temperatures over a range of undercoolings 30 to 2 K below T_M. After 4.2 ns equilibration runs at each temperature, statistics were obtained for w at a given temperature as follows. For each snapshot (selected at a frequency of 10 ps) w is determined by utilizing the scheme developed in the capillary fluctuation method [17]. Each atom is assigned a structural order parameter ϕ_i constructed from the positions of the 12 nearest neighbor atoms, and the ϕ_i values are then averaged in bins along the direction normal to the boundary. The point of inflection in the average order parameter profile is taken as the position of one of the solid-liquid interfaces. The procedure is repeated to locate the second solid-liquid interface and hence the GB width.

An important observation in the present work is that the width of the GB regions is highly dynamic in the MD simulations, particularly at the temperatures closest to T_M. This point is illustrated clearly in Fig. 2 which shows three snapshots, taken from a 40 ns simulation at an undercooling of 2 K, where the atoms have been color coded based on their ϕ_i values, blue representing a liquidlike environment and red the crystal. The snapshots clearly demonstrate the presence of large fluctuations in the width of the premelted layer over the course of the simulation. The highly dynamic nature of the premelted layer provides a framework for extracting the disjoining potential. We show in Fig. 3 histograms of interface width obtained at five temperatures near the melting point. The solid lines represent least-squares fits to the data employing the thermodynamic model of Eq. (1) as follows. The probability $[P(w)]$ of observing a premelted layer width w is given as

$$P(w) = C \exp[-AG(w)/k_BT], \tag{3}$$

where C is a temperature-dependent normalization constant, A is the cross-sectional area, and $G(w)$ is defined in Eq. (1). The data in Fig. 1 suggests a logarithmic divergence of w with increasing temperature, and in order to fit Eq. (3) to the MD data, we therefore employ the form for the disjoining potential given in Eq. (2). The least-squares fits of $P(w)$ versus w for all five undercoolings studied are shown in Fig. 3. The excellent agreement suggests that the free energy of Eq. (1) together with the disjoining potential [Eq. (2)] represents an accurate model for the premelting behavior of this boundary. The analysis of Fig. 3 assumed a melting point of $T_M = 1710$ K. If instead a value of just 1 K different, i.e., $T_M = 1709$ K, is assumed, then a poor fit to $P(w)$ is obtained at the lowest undercooling. In addition, for simulations run at a temperature of 1712 K the system exhibited a gradual melting. These findings, together with the results of separate coexistence simulations, indicate that the melting temperature is known to a precision approaching ± 1 K.

As an independent check on the validity of Eq. (2), we employ an additional analysis of the data of Fig. 3. From Eq. (3) the disjoining potential can be written in terms of $P(w)$ as

$$\Psi(w) = -(k_BT/A)\ln P(w,T_i) - \Delta G_f w + a_i, \tag{4}$$

where the a_i are unknown constants related to C in Eq. (3) and the subscript i denotes a separate histogram of data corresponding to each undercooling. The a_i can be determined by a least-squares fitting procedure such that all the data sets can be merged and the entire function $\Psi(w)$ constructed. Notice that the procedure adopted here is analogous to the histogram method, often employed in Monte Carlo simulations to extract transition states and energy barriers, but with the undercooling playing the role of a bias potential. The results of the histogram procedure are shown in Fig. 3. The inset of the figure plots the right-hand side of Eq. (4), with all the constant terms a_i set to zero to illustrate that different undercoolings sample a range of w regimes of $\Psi(w)$. The main figure shows the final $\Psi(w)$ function along with a fit (solid line) to the exponential form given in Eq. (2). It is important to note that the fit parameters obtained via the histogram method ($\delta = 2.49$ Å and $\Delta\gamma = 156$ mJ/m^2) compare

very well to those derived through the individual fits of the separate histograms in Fig. 3: $\delta=2.67\pm0.18$ Å and $\Delta\gamma=127\pm26$ mJ/m^2.

The present simulations have quantified only the short-ranged contribution to $\Psi(w)$. However, for setting the temperature scale over which premelting can be observed in elemental metals, we estimate that this is the dominant contribution. For values of $w\sim1$ nm we can estimate an upper bound on the dispersion forces using a value of the Hamaker constant measured for surface premelting of metals [14]. This gives a contribution to $\Psi(w=1\text{ nm})\sim0.4$ mJ/m^2, approximately one order of magnitude smaller than the results presented in Fig. 4, computed from the value of Ψ_{SR} using the parameters derived above.

Thus, for high-energy boundaries it can be expected that the lowest temperature where premelting will become appreciable is set through the relation $(\Delta T/T_M)=(\Delta\gamma/L\rho\delta)\exp(-w_{eq}/\delta)$, with $w_{eq}\sim1$ nm, where we have expressed $\Delta G_f=L\Delta T\rho/T_M$ in terms of the latent heat per atom (L), the solid density (ρ), and the undercooling ($\Delta T=T_M-T$). The present results give δ on the order of an interatomic spacing and $\Delta\gamma$ on the order of half γ_{SL}. While the exact values will vary somewhat depending on the system, we believe these values are well representative of high-energy boundaries in pure metals. With these estimates we obtain a value of ΔT required to obtain $w\sim1$ nm of $(\Delta T/T_M)\sim(\alpha/2)\exp(-4)$, where we have used $\rho\delta^{1/3}\sim1$ and the relation $\gamma_s l\rho^{-2/3}/L=\alpha$, where α is the Turnbull coefficient [20], which has a roughly constant value of about 0.5 for elemental metals [17]. The estimate of the undercooling required for a 1 nm premelted film is thus $\Delta T/T_M\sim0.005$. The results are consistent with the experimental studies of Balluffi and co-workers [3], who estimated a lower bound of $T=0.999T_M$ for the temperature where boundary widths of a few nanometers could be observed experimentally.

J.J.H. acknowledges financial support from a Natural Sciences and Engineering Research Council (NSERC) of Canada Discovery grant. Work at U.C. Davis and Northeastern was supported by the U.S. Department of Energy (DOE), Office of Basic Energy Sciences, under Contracts No. DE-FG02-01ER45910 and No. DE-FGO2-07ER46400, respectively. Sandia is a multiprogram laboratory operated by Sandia Corporation, a Lockheed Martin Company, for the DOE's National Nuclear Security Administration under Contract No. DE-AC04-94AL85000. M.A. and S.J. acknowledge helpful discussions with Dr. R. G. Hoagland. All the authors acknowledge support from the DOE Computational Materials Science Network program.

[1] F. Inoko, T. Okada, T. Nishimura, M. Ohomori, and T. Yoshimura, Interface Sci. **7**, 131 (1999); S. Divinski, M. Lohmann, C. Herzig, B. Straumal, B. Baretzky, and W. Gust, Phys. Rev. B **71**, 104104 (2005); J. Luo, V. K. Gupta, D. H. Yoon, and H. M. Meyer III, Appl. Phys. Lett. **87**, 231902 (2005).

[2] M. E. Glicksman and C. L. Vold, Surf. Sci. **31**, 50 (1972); S. Sasaki, F. Caupin, and S. Balibar, Phys. Rev. Lett. **99**, 205302 (2007); A. M. Alsayed, M. F. Islam, J. Zhang, P. J. Collings, and A. G. Yodh, Science **309**, 1207 (2005).

[3] S.-W. Chan, J. S. Liu, and R. W. Balluffi, Scr. Metall. **19**, 1251 (1985); T. E. Hsieh and R. W. Balluffi, Acta Metall. **37**, 1637 (1989).

[4] R. Lipowsky, Phys. Rev. Lett. **57**, 2876 (1986).

[5] D. R. Clarke, J. Am. Ceram. Soc. **70**, 15 (1987).

[6] B. Widom, J. Chem. Phys. **68**, 3878 (1978).

[7] R. Lipowsky and M. E. Fisher, Phys. Rev. B **36**, 2126 (1987).

[8] D. S. Fisher and D. A. Huse, Phys. Rev. B **32**, 247 (1985).

[9] R. Kikuchi and J. W. Cahn, Phys. Rev. B **21**, 1893 (1980).

[10] A. E. Lobkovsky and J. A. Warren, Physica D **164**, 202 (2002).

[11] M. Tang, W. C. Carter, and R. M. Cannon, Phys. Rev. Lett. **97**, 075502 (2006).

[12] J. Mellenthin, A. Karma, and M. Plapp, Phys. Rev. B **78**, 184110 (2008).

[13] J. Berry, K. R. Elder, and M. Grant, Phys. Rev. B **77**, 224114 (2008).

[14] B. Pluis, T. N. Taylor, D. Frenkel, and J. F. van der Veen, Phys. Rev. B **40**, 1353 (1989).

[15] G. Ciccotti, M. Guillope, and V. Pontikis, Phys. Rev. B **27**, 5576 (1983); F. Carrion, G. Kalonji, and S. Yip, Scr. Metall. **17**, 915 (1983); T. Nguyen, P. S. Ho, T. Kwok, C. Nitta, and S. Yip, Phys. Rev. Lett. **57**, 1919 (1986); P. Deymier, A. Taiwo, and G. Kalonji, Acta Metall. **35**, 2719 (1987); J. Q. Broughton and G. H. Gilmer, Phys. Rev. Lett. **56**, 2692 (1986); J. F. Lutsko, D. Wolf, S. Yip, S. R. Phillpot, and T. Nguyen, Phys. Rev. B **38**, 11572 (1988); V. Pontikis, J. Phys. Colloq. **49**, 327 (1988); T. Nguyen, P. S. Ho, T. Kwok, C. Nitta, and S. Yip, Phys. Rev. B **46**, 6050 (1992); S. R. Phillpot, J. F. Lutsko, D. Wolf, and S. Yip, *ibid.* **40**, 2831 (1989); J. Q. Broughton and G. H. Gilmer, Modell. Simul. Mater. Sci. Eng. **6**, 87 (1998); W. Fan and X.-G. Gong, Phys. Rev. B **72**, 064121 (2005).

[16] S. von Alfthan, K. Kaski, and A. P. Sutton, Phys. Rev. B **76**, 245317 (2007).

[17] J. J. Hoyt, M. Asta, and A. Karma, Mater. Sci. Eng. R. **41**, 121 (2003).

[18] S. M. Foiles, M. I. Baskes, and M. S. Daw, Phys. Rev. B **33**, 7983 (1986).

[19] D. Y. Sun, M. Asta, and J. J. Hoyt, Phys. Rev. B **69**, 024108 (2004).

[20] D. T. Turnbull, J. Appl. Phys. **21**, 1022 (1950).